Binding of the Dimeric Deinococcus radiodurans Single-Stranded DNA Binding Protein to Single-Stranded DNA

ARTICLE *in* BIOCHEMISTRY · SEPTEMBER 2010

Impact Factor: 3.02 · DOI: 10.1021/bi100920w · Source: PubMed

4 AUTHORS, INCLUDING:

Alexander G Kozlov
Washington University in St. Louis
34 PUBLICATIONS **1,367** CITATIONS
SEE PROFILE

Michael M Cox
University of Wisconsin–Madison
210 PUBLICATIONS **12,874** CITATIONS
SEE PROFILE

Timothy M. Lohman
Washington University in St. Louis
189 PUBLICATIONS **12,037** CITATIONS
SEE PROFILE

Published in final edited form as:
Biochemistry. 2010 September 28; 49(38): 8266–8275. doi:10.1021/bi100920w.

Binding of the Dimeric *Deinococcus radiodurans* SSB Protein to Single-stranded DNA†

Alexander G. Kozlov[1], **Julie M. Eggington**[2], **Michael M. Cox**[2], and **Timothy M. Lohman**[1,*]

[1]Department of Biochemistry and Molecular Biophysics, Washington University School of Medicine, 660 S. Euclid Ave., St. Louis, MO 63110

[2]Department of Biochemistry, University of Wisconsin-Madison, 433 Babcock drive, Madison, Wisconsin 53706-1544

Abstract

D. radiodurans single stranded (ss) DNA binding protein (*Dr*SSB) originates from a radiation-resistant bacterium and participates in DNA recombination, replication and repair. Although it functions as a homodimer, it contains four DNA binding domains (OB folds) and thus is structurally similar to the *E. coli SSB* (*Eco*SSB) homotetramer. We examined the equilibrium binding of *Dr*SSB to ssDNA to compare with *Eco*SSB. We find that the occluded site size of *Dr*SSB on poly(dT) is ~45 nucleotides in low salt (<0.02M NaCl) but increases to 50–55 nucleotides at [NaCl] ≥ 0.2M. This suggests that DrSSB undergoes a transition between ssDNA binding modes as is observed for *Eco*SSB, although the site size difference between modes is not as large as for *Eco*SSB, suggesting that the pathways of ssDNA wrapping differ for these two proteins. The occluded site size corresponds well to the contact site size (52 nucleotides) determined by Isothermal Titration Calorimetry (ITC). Electrophoretic studies of complexes of *Dr*SSB with phage M13ssDNA indicate the formation of stable, highly cooperative complexes at low salt conditions. Using ITC we find that *Dr*SSB binding to oligo(dT)s with lengths close to the determined site size (50–55 nts) is stoichiometric with ΔH_{obs} ≈-94±4 kcal/mole, somewhat smaller than for *Eco*SSB (≈-130 kcal/mole) under the same conditions. The observed binding enthalpy shows a large sensitivity to NaCl concentration, similar to that observed for *Eco*SSB. With the exception of the less dramatic change in occluded site size, the behavior of *Dr*SSB is similar to that of *Eco*SSB protein (although, clear quantitative differences exist). These common features for SSB proteins having multiple DNA binding domains enable versatility of SSB function *in vivo*.

Single-stranded DNA binding proteins are essential in nearly all organisms and play central roles in all aspects of genome maintenance, including DNA replication, recombination and repair (1–3). They bind selectively single stranded DNA with high affinity and independent of sequence specificity, protecting ssDNA intermediates from degradation and preventing them from the formation of secondary structures. The other functions of SSB proteins have become recognized only recently and include the regulation of the activity of many other DNA metabolic proteins through direct protein-protein interactions (4) as well as by modulating the accessibility of ssDNA by either different modes of binding (3,5) or by the ability to translocate along ssDNA as shown recently for *EcoSSB* (6). Although SSB proteins from different organisms can differ in architecture, for example, the bacteriophage T4 gene 32 protein is a monomer (7,8), *EcoSSB* protein is a homotetramer (9–11) and eucaryotic RPA proteins are

†This research was supported in part by the NIH (GM30498 to TML and GM32335 to MMC)

*Address correspondence to: Department of Biochemistry and Molecular Biophysics, Box 8231, Washington University School of Medicine, 660 South Euclid Ave., St. Louis, M0 63110, lohman@biochem.wustl.edu, Tel: (314)-362-4393, FAX: (314)-362-7183.

heterotrimers (12,13), they all contain oligonucleotide/oligosaccharide binding folds (OB-fold), which form the primary site for ssDNA binding (14,15). The number of OB folds varies significantly in these proteins, from one in T4 gene 32 protein to six in the hetero-trimeric RPAs. Most of the bacterial SSBs are homotetramers and contain 4 OB-folds (one per monomer) (see for example (16–19), with the *EcoSSB* tetramer being the most studied. In contrast to the homotetrameric SSB proteins, SSB proteins from *Deinococcus-Thermus* group function as homodimers; however, each monomer encodes two OB-folds linked by a conserved spacer sequence (20–23). Therefore, the functional form of these proteins still is composed of four OB-folds, although the sequence differences between the two OB-folds within each dimer impose an asymmetry that is likely to affect its DNA binding properties. Furthermore, these dimers possess only two unstructured C-termini, rather than four as is the case for the homo-tetrameric SSB proteins.

DrSSB protein originates from one of the most radiation resistant organisms known (24). *D. radiodurans*, which is a soil bacterium featuring a D_{37} γ irradiation dose of approximately 6,000 Gy, making this organism roughly 200 times more radiation resistant than *Escherichia coli* (24). DrSSB forms a stable homodimer in solution (22) and its quantitative estimates in the *D. radiodurans* cell indicate approximately 2500–3000 dimers/cell, independent of the level of irradiation (25).

A crystal structure of the full length DrSSB was determined with 1.8A resolution (23) and shows that each DrSSB subunit comprises two OB-folds linked by a β-hairpin motif and the protein assembles a four-OB-fold arrangement by means of symmetric dimerization. The C-terminal tail residues 234–301 are missing from the model due to the lack of electron density suggesting that the extended C-terminal region of this protein is highly unstructured similar to the C-terminal tails of *EcoSSB* (11).

In order to better understand the functional consequences arising from these differences, we have examined the binding of *Deinococcus radiodurans* SSB (DrSSB) to a variety of ssDNA to compare its DNA binding properties with those of the well-studied homo-tetrameric *EcoSSB*.

MATERIALS AND METHODS

Reagents and Buffers

Buffers were prepared with reagent grade chemicals and distilled water that was subsequently treated with a Milli Q (Millipore, Bedford, MA) water purification system. Buffer T is 10 mM Tris, pH8.1, and buffer P is 10 mM Phosphate pH 7.0. All buffers contained 0.1 mM Na_3EDTA and 1mM BME. The concentrations of NaCl used in the experiments are specified in the text.

DrSSB and ssDNA

*Dr*SSB protein was expressed and purified as described (22,26) and its concentration determined spectrophotometrically in Tris buffer (pH 8.1, 0.2 M NaCl) using an extinction coefficient of $8.2\times10^4\ M^{-1}\ cm^{-1}$ (dimer) (22). Single-stranded circular phage M13 mp18 DNA was purchased from New England Biolabs, Inc. (Ipswich, MA). The oligodeoxynucleotides, $(dT)_L$, (L=30,35,40,45,50,55,60,70) were synthesized and purified as described (27) and were ≥ 98% pure as judged by denaturing gel electrophoresis and autoradiography samples that was 5′ end-labeled with ^{32}P using polynucleotide kinase. The poly(dT) (Midland Certified Reagent Co., Midland, TX) had an average length of ~1100 nucleotides. Concentrations of nucleic acids were determined spectrophotometrically in buffer T (pH 8.1), 100 mM NaCl using an extinction coefficient $\varepsilon_{260}=8.1\times10^3\ M^{-1}$ (nucleotide) cm^{-1} for oligo(dT) and poly(dT) (8) and $\varepsilon_{259}=7370\ M^{-1}$ (nucleotide) cm^{-1} for single stranded M13 ssDNA (28).

Fluorescence titrations

Equilibrium binding of DrSSB protein to oligodeoxynucleotides, $(dT)_L$ and poly(dT) was performed by monitoring quenching of the intrinsic Trp fluorescence of DrSSB upon addition of ssDNA using a PTI QM-2000 spectrofluorometer (Photon Technologies, Inc., Lawrenceville, NJ) [λ_{ex}=296 nm (2 nm excitation band-pass) and λ_{em}=345 nm (2–4 nm emission band-pass)] with corrections applied as described (29,30). The binding isotherms shown in Fig. 2 for the interaction of $(dT)_L$ (L=45,50 and 55) (X, ligand) with DrSSB dimer (M, macromolecule) were analyzed with a 1:1 binding model using eq. 1:

$$Q_{obs}=\frac{Q_{\max} n \cdot K_{obs} X}{1+K_{obs} D} \quad (1)$$

where Q_{obs} is the observed fluorescence quenching and Q_{max} is a fluorescence quenching at saturation; n and K_{obs} are the stoichiometry of binding and equilibrium association constant. The concentration of free $(dT)_L$, X, was determined from the mass conservation equation 1a:

$$X_{tot}=M+X_{bound}=X+\frac{n \cdot K_{obs} X}{1+K_{obs} X} M_{tot} \quad (1a)$$

The binding isotherms shown in Fig. 3 for the interaction of two $(dT)_{25}$ molecules (ligand, X) with DrSSB dimer (macromolecule, M) were analyzed using a two-site sequential binding model and eq. 2:

$$Q_{obs}=\frac{Q_1 K_{1,obs} X+Q_2 K_{1,obs} K_{2,obs} X^2}{1+K_{1,obs} X+K_{1,obs} K_{2,obs} X^2} \quad (2)$$

where Q_{obs} is the observed fluorescence quenching and Q_1 and Q_2 are the fluorescence quenchings corresponding to one and two $(dT)_{25}$ molecules bound, respectively; $K_{1,obs}$ and $K_{2,obs}$ are the observed step-wise macroscopic association constants for the binding of the first and the second DNA molecule. The concentration of free DNA, X, was determined from the mass conservation equation 2a:

$$X_{tot}=X+X_{bound}=X+\frac{K_{1,obs} X+2K_{1,obs} K_{2,obs} X^2}{1+K_1 X+K_{1,obs} K_{2,obs} X^2} M_{tot} \quad (2a)$$

In eqs 1 and 2 X_{tot} and M_{tot} are total concentrations of the $(dT)_{25}$ and the protein, respectively. The fitting of the data were performed using the nonlinear regression package in Scientist (MicroMath Scientist Software, St. Louis, MO).

Isothermal Titration Calorimetry (ITC)

ITC experiments were performed using a VP-ITC titration microcalorimeter (MicroCal Inc., Northhampton, MA) (31). Generally, experiments were carried out by titrating DrSSB (1–2μM (dimer) in the cell) with oligo(dT) solutions (10–25 μM in the syringe). The heats of dilution were usually obtained from a reference titration in which the species in the syringe is titrated into the cell containing only buffer solution. All corrections for heats of dilution were applied as described (32). Oligo(dT) and protein samples were dialyzed extensively vs. the buffer containing the indicated salt concentration used in the ITC experiments.

The DrSSB binds one molecule of $(dT)_L$, when L=35,40,45,50,55 and 60. The stoichiometry of binding, n, and the values of K_{obs} (where measurable) and ΔH_{obs} were obtained by fitting the ITC titration curves to a model of ligand (X= $(dT)_L$) binding to n-identical and independent sites on the macromolecule (M=DrSSB) using eq. 3,

$$Q_i^{tot}=V_0 \cdot \Delta H_{obs} \cdot M_{tot} \cdot \frac{nK_{obs}X}{1+K_{obs}X} \quad (3)$$

where Q_i^{tot} is the total heat after the *i*-th injection and V_0 is the volume of the calorimetric cell. The concentration of free ligand (X) was obtained by solving eq. 1a. When the length of $(dT)_L$ is shorter than 35 nucleotides, or longer than 60 nucleotides the observed binding isotherms display two-step behavior indicative of weak binding of a second $(dT)_L$ molecule (X) to DrSSB (M) (when L<35) or a second DrSSB dimer (X) to $(dT)_L$ (macromolecule M) (when L>60), respectively. For these cases we used a 2 site sequential binding model, characterized by two macroscopic binding constants ($K_{1,obs}$ and $K_{2,obs}$) and two binding enthalpies ($\Delta H_{1,obs}$ and $\Delta H_{2,obs}$) as described by eq. 4,

$$Q_i^{tot}=V_0 \cdot \Delta H_{obs} \cdot M_{tot} \cdot \left(\frac{K_{1,obs}X \cdot \Delta H_{1,obs}+K_{1,obs}K_{2,obs}X^2 (\Delta H_{1,obs}+\Delta H_{2,obs})}{1+K_{1,obs}X+K_{1,obs}K_{2,obs}X^2} \right) \quad (4)$$

where the concentration of free ligand (X) was obtained by solving eq. 2a. In eqs 3 and 4 X_{tot} and M_{tot} are the total concentrations of the ligand and macromolecule, respectively, in the calorimetric cell after the *i*-th injection. Non-linear least squares fitting of the data was performed using the "ITC Data Analysis in Origin" software provided by the manufacturer.

The conversion of integral heats (Q_i^{tot}) to differential heats (heats per injection observed in the experiment) and the fitting routine including corrections for heat displacement effects and ligand and macromolecule dilutions in the calorimetric cell were performed as described (32) (see also the *ITC Data Analysis in Origin Tutorial Guide* (Microcal Inc.)). Additional fittings and simulations were also performed using the nonlinear regression package in Scientist (MicroMath Scientist Software, St. Louis, MO).

Agarose gel electrophoresis of DrSSB-ssM13 DNA complexes

The distribution of DrSSB molecules bound to circular phage M13 ssDNA was monitored by separating the DNA molecules by gel electrophoresis based on the amount of DrSSB bound using 0.5% agarose gels as described (33). In these experiments the amount of DNA loaded into each lane was held constant ≈1.5 nmole (nucleotides) while the amount of DrSSB in the solution was varied from 0 to 0.03 nmole (dimer) in order to saturate the M13mp8 with DrSSB, assuming that DrSSB binding site size is 45–50 nucleotides. The complexes were formed in buffer T (10 mM Tris, pH 8.1, 0.1mM EDTA) at two NaCl concentrations (0.02M and 0.3M); the total reaction volume of each sample was 30 µl. The time of incubation was varied as noted in the text. The electrophoresis running buffer was 20 mM Tris-Acetate (pH 8.1), 0.5 mM Na_3EDTA. Loading dye (2 µl of 50% (v/v) glycerol, 0.04% (w/v) bromophenol blue) was added to each 30 µl sample. Electrophoresis was carried out at room temperature (22° C) at constant voltage (8 V/cm) for ~3 hours. The gels were then stained for 15 min with ethidium bromide (2 µg/ml solution) and destained for 2 hours at 4° C in buffer T + 1 M NaCl.

RESULTS

Occluded ssDNA binding site size of DrSSB on poly(dT)

Characterization of the ssDNA binding properties of a nonspecific ssDNA binding protein such as DrSSB requires a determination of the occluded site size (n), defined as the number of ssDNA nucleotides that are occluded by one protein and thus prevented from interacting with a second protein (34). For oligomeric SSB proteins containing multiple OB folds and thus potential sites for ssDNA binding the occluded site size will be affected by the number of OB-folds that are involved in the interaction. For example, the *Eco*SSB homotetramer, possessing four OB-folds (one per subunit), can bind ssDNA in multiple binding modes. Two of the major binding modes differ in that ssDNA occupies either two or four subunits with corresponding occluded site sizes of ~35 and 65 nucleotides (3,35). Both modes involve at least partial wrapping of ssDNA around the tetramer (10). The relative populations of these binding modes are influenced by protein binding density, salt type and valence and salt concentration (5,35–39) with the SSB_{35} binding mode preferred at low salt (<0.02M NaCl) and high protein binding densities, and the SSB_{65} binding mode favored at high salt (≥0.2M NaCl). Similar effects have been observed for the *Saccaromyces cerivisiae* (sc)RPA where the occluded site size increases from ~18 nucleotides at low salt to ~27 nucleotides at high salt as a result of the interaction of ssDNA with an additional OB-fold within scRPA heterotrimer (40).

We measured the occluded site size for the DrSSB dimer binding to the homopolynucleotide poly(dT) as a function of salt concentration to determine if multiple ssDNA binding modes could be detected for this protein. The results of DrSSB titrations with poly(dT) at different NaCl concentrations (Tris-buffer, pH 8.1, 25°C), monitoring the quenching of drSSB tryptophan fluorescence, are presented in Fig. 1 and Table 1. In the absence of added salt and at low [NaCl] concentration (20mM) (see Fig. 1A), the Trp fluorescence quenching increases linearly with increasing poly(dT) concentration, reaching a quenching plateau of 72% (no salt added) and 76% (20mM NaCl) at saturating poly(dT). The intersection of the initial linear region with the plateau occurs at n≈45 nucleotides per DrSSB dimer providing an estimate of the occluded site size of the DrSSB dimer on poly(dT). The observed stoichiometries were independent of DrSSB concentration (titrations performed at 70 and 200 nM DrSSB), indicating that binding is stoichiometric under these conditions. Similar stoichiometric binding is observed at 0.2M and 0.5M NaCl (see Fig. 1B); however, both the occluded site size and the maximum Trp fluorescence quenching increase to n≈50–55 and 83–84%, respectively. Titrations performed at a still higher [NaCl] of 1 M results in a binding isotherm indicating that binding is no longer stoichiometric (Fig. 1B), making it impossible to determine an occluded site size by the extrapolation method. Thus, binding at 1 M NaCl is no longer stoichiometric. This is different from what is observed for the binding of *Eco*SSB with poly (dT), where binding remains stoichiometric up to 3M NaCl and is characterized by an occluded site size n≈65 with 90–92% quenching (36). Hence, DrSSB appears to have a smaller high salt occluded site size and lower affinity for poly(dT) compared to *Eco*SSB.

As a further test of whether the high [NaCl] site size of the DrSSB dimer on ssDNA does not exceed 50–55 nucleotides we performed titrations of DrSSB with oligodeoxythymidylates of different length ($(dT)_L$, L=45, 50 and 55 nucleotides) at different NaCl concentrations (buffer-T, pH 8.1, 25°C). Fig.2 and Table 1 show the results obtained at 0.2M NaCl indicating that DrSSB dimer binds one molecule of $(dT)_{45}$, $(dT)_{50}$ or $(dT)_{55}$, stoichiometrically as expected based on the DrSSB-poly(dT) results. Furthermore, the extent of Trp fluorescence quenching is ~74% for $(dT)_{45}$, but increases to 83–85% for both $(dT)_{50}$ and $(dT)_{55}$ consistent with a high [NaCl] site size of ~ 50 nucleotides. Titrations performed at a lower [NaCl] (0.02M NaCl (data not shown)) also show stoichiometric binding behavior with quenching values of ~76% for $(dT)_{45}$ and ~84–85% for $(dT)_{50}$, $(dT)_{55}$). The results of the titrations of DrSSB with the different $(dT)_L$ suggests that the different behavior observed for DrSSB binding to poly(dT) reflects a

real difference in the mode of ssDNA binding, possible reflecting a difference in the mode of ssDNA wrapping and/or inter-dimer protein-protein cooperativity (see Discussion). It is also clear from the isotherm in Fig. 2B that in 1M NaCl $(dT)_{45}$ interacts with DrSSB much more weakly than at lower [NaCl]. The titration curve in Fig. 2B can be fitted to an n-identical-independent sites model (eq. 1, Materials and Methods) with the following parameters, n=0.98 ±0.02, Q_{max}=0.73±0.01, K=(1.48±0.06)×10^7 M^{-1}. This suggests that the more shallow isotherm observed in the titration of DrSSB with poly(dT) at 1M NaCl (Fig. 1B) reflects a lower affinity due to the increase in NaCl concentration.

DrSSB binds two molecules of $(dT)_{25}$ with a [NaCl]-dependent negative cooperativity

The *EcoSS*B tetramer displays intra-tetramer negative cooperativity for binding two molecules of $(dT)_{35}$ and this negative cooperativity is a strong function of salt concentration (41,42). Each subunit of DrSSB dimer contains two OB folds and thus we wanted to determine whether a similar negative cooperativity might exist for ssDNA binding to the DrSSB dimer. Assuming that the full occluded site size for ssDNA binding to the DrSSB dimer is ~50 nucleotides we examined the equilibrium binding of two molecules of $(dT)_{25}$ to the DrSSB dimer. Figure 3A and 3B shows the results of equilibrium titrations of DrSSB with $(dT)_{25}$, monitoring Trp fluorescence at low (0.02M NaCl) and moderate (0.2M NaCl) salt concentrations (Tris buffer, pH 8.1, 25°C), respectively. From these results it is clear that at both salt concentrations the second molecule of $(dT)_{25}$ binds with weaker affinity than the first molecule, indicating negative cooperativity. Furthermore, the binding of the first $(dT)_{25}$ to DrSSB occurs with much stronger affinity at the lower [NaCl]. In order to estimate the binding parameters we used a 2-site sequential binding model (see eq. 2 in Materials and Methods) with two macroscopic binding constants $K_{1,obs}$ and $K_{2,obs}$ for the first and the second site with Q_1 and Q_2 characterizing the extent of DrSSB Trp quenching for one and two molecules of $(dT)_{25}$ bound, respectively. For each salt concentration we globally fit two titration curves by constraining Q_2 = 0.83 corresponding to the maximum fluorescence quenching observed upon binding poly (dT) and $(dT)_{50}$. The following parameters were obtained: Q_1 = 0.48±0.01, K_1 =(4.5±6.2) ×10^9 M^{-1}, K_2 =(1.4±0.1)×10^5 M^{-1}, for 20mM NaCl and Q_1 = 0.51±0.01, K_1 =(3.1±0.6) ×10^7 M^{-1}, K_2 =(2.1±0.3)×10^5 M^{-1}, for 0.2M NaCl. Interestingly the affinity for binding the first $(dT)_{25}$ to DrSSB decreases by more than a factor of 100 as the salt concentration increases 10 fold, whereas the binding of the second $(dT)_{25}$ is essentially unchanged. In general this observed decrease in negative cooperativity with increasing [NaCl] follows the same trend as observed for the *EcoSSB* tetramer (41,42).

Calorimetric determination of DrSSB contact site size

The contact site size, *m*, is defined as a number of contiguous nucleotides required to form all interactions with the protein. This may differ from the occluded site size, *n*, which is a measure of the number nucleotides that are occluded by one protein molecule upon binding to ssDNA, such that the second protein molecule is unable to access these nucleotides, therefore, $m \leq n$. In order to estimate the contact site size for DrSSB binding to ssDNA we performed ITC titrations of DrSSB with the a series of $(dT)_L$ (L=30, 35, 40, 45, 50, 55, 60, 70 nucleotides) at 0.2M NaCl (buffer T, pH 8.1, 25°C) to determine how the equilibrium binding constant (K_{obs}) and the binding enthalpy (ΔH_{obs}) are affected by L. The magnitude of ΔH_{obs} is expected to increase as the number of nucleotides involved in the protein interaction increases until *m* is reached.

Figure 4 shows a series of representative ITC isotherms for experiments in which $(dT)_L$ was titrated into DrSSB (0.5–0.8 μM) in conditions mentioned above. These isotherms indicate that when $40 \leq L \leq 60$ nucleotides, the DrSSB dimer binds one molecule of $(dT)_L$ stoichoiometrically, so that the equilibrium binding constant cannot be determined due to the very high affinity (K_{obs}>10^9 M^{-1}). Under these conditions only the binding enthalpy (ΔH_{obs})

can be estimated reliably. When L is less than 35 nucleotides an interaction of a second molecule of $(dT)_L$ with DrSSB can be detected, although this binds with much weaker affinity (see Fig. 4). At the same time, weak binding of a second DrSSB dimer to $(dT)_L$ becomes detectable when the length of oligo(dT) exceeds the binding site size (e.g., see $L \geq 70$ nucleotides in Fig. 4). Although in both cases determination of the binding parameters for the second molecule of $(dT)_L$ or DrSSB is not reliable, the estimates of the binding enthalpy for the first molecule ($\Delta H_{1,obs}$) can be obtained accurately. The inset to Figure 4 shows that the values of ΔH_{obs} for the interaction of DrSSB with one molecule of $(dT)_L$ are all negative and increase in magnitude linearly with increasing L up to L≈52 nucleotides leveling off at ΔH_{obs} = 94±4 kcal/mol for L >50. These data allow an estimate of m≈52 nucleotides for the contact site size, which is the same as the estimate of the occluded site size obtained from fluorescent experiments with poly (dT) under the same conditions.

Salt and temperature dependencies of the interaction of DrSSB with $(dT)_{45}$

Solution conditions and salt concentration and type have significant effects on the magnitude of binding enthalpy (ΔH_{obs}) for the binding of the *Eco*SSB tetramer to ssDNA (32,43) as well as on its temperature dependence (ΔCp_{obs}) (44). These effects are linked primarily to the release of anions from *Eco*SSB upon ssDNA binding (44). In order to investigate the generality of these effects we examined the interaction of *Dr*SSB with ssDNA at different NaCl concentrations and temperatures using ITC.

Fig.5A shows the results of 1:1 binding of *Dr*SSB to $(dT)_{45}$ at different NaCl concentrations (buffer T, pH 8.1, 25°C). The binding is stoichiometric at 0.02M and 0.2M NaCl, but is weakened at 1 M NaCl. Hence, a determination of both ΔH_{obs} and K_{obs} is possible at 1 M NaCl, and the estimated value of K_{obs}=(1.7±0.1)×10^7 M^{-1} is in a good agreement with the value determined by monitoring Trp fluorescence (K_{obs}=(1.5±0.1)×10^7 M^{-1}, see Fig. 2B). The ΔH_{obs} values are all negative, but exhibit a nonlinear decrease in magnitude as a function of [NaCl] (see inset in Fig. 5A). This overall dependence of ΔH_{obs} on [NaCl] is very similar to that observed for *Eco*SSB binding to $(dT)_{70}$ (32) indicating large effect of salt on ΔH_{obs}.

We next examined the temperature dependence of ΔH_{obs} for *Dr*SSB binding to $(dT)_{45}$ in 0.2M NaCl (buffer P, pH 7.5) (see Figure 5B). Phosphate buffer was used since it has a very low ionization enthalpy and thus minimizes the potential contributions to ΔH_{obs} from any protonation events that may accompany ssDNA binding as has been observed for *Eco*SSB (45). Figure 5B shows that ΔH_{obs} becomes more negative with increasing temperature. Linear least square analysis of the data in Figure 5B yields a value of ΔCp_{obs} = −290 ± 70 cal/mol deg which is approximately four times smaller in magnitude than that measured for the *Eco*SSB-$(dT)_{70}$ interaction under similar conditions (44)

Cooperativity of DrSSB binding to M13ssDNA probed by agarose gel electrophoresis

Single-stranded binding proteins have been observed to bind long ssDNA cooperatively under some conditions to form extended protein clusters. The T4 gene 32 protein binds ssDNA with high cooperativity independent of solution conditions (7,8). On the other hand the *Eco*SSB tetramer only binds ssDNA with high cooperativity in its $(SSB)_{35}$ binding mode (27,33,37–39,46) which is favored at low monovalent salt concentrations and high protein/DNA ratios. In contrast, the fully wrapped $(SSB)_{65}$ binding mode which dominates at high salt concentrations displays little cooperativity (33,37,46–48). We were therefore interested to determine if *Dr*SSB binds to ssDNA with detectable cooperativity and whether salt concentration influences this cooperativity. In general such information can be described in terms of intrinsic binding constant (K) and a nearest neighbor cooperativity parameter (ω) using the models of protein binding to infinite (34,49,50) or finite lattices (51). Unfortunately, under most conditions (up to 0.5 M NaCl) the binding of *Dr*SSB to poly(dT) is stoichiometric so that

accurate determination of the affinity (K) and cooperativity (ω) is not possible. Therefore in order to investigate this we used an agarose gel electrophoresis assay as used in studies of the cooperativity of *Eco*SSB binding to M13ssDNA (33).

We examined the binding cooperativity of DrSSB to circular M13ssDNA using an agarose gel electrophoresis assay at two different NaCl concentrations (0.02 and 0.3M). The complexes were formed at varying *Dr*SSB to DNA ratios by directly mixing the *Dr*SSB and M13ssDNA in buffer T, pH 8.1, and equilibrating for one hour before electrophoresis (see Materials and Methods). At 0.3 M NaCl (Figure 6A) the ssDNA patterns show a single, somewhat diffuse band at each DrSSB concentration indicating that all ssDNA molecules have close to the same DrSSB binding densitiy consistent with low cooperativity of *Dr*SSB binding to M13ssDNA. However, at 0.02 M NaCl (Figure 6B) the ssDNA pattern shows a bimodal distributions at intermediate saturation levels (lines 5 and 6, in particular, with 20 and 30% saturation of DNA) indicating of high degree of cooperativity. These non-random binding density distributions at low *Dr*SSB to DNA ratios indicate the presence of ssDNA that has high amounts of *Dr*SSB bound in the same population with ssDNA that has much lower amounts of *Dr*SSB bound. At higher ratios of *Dr*SSB to DNA (≥50% saturation, lanes 8–11) only single bands are observed indicating a fairly uniform population of highly saturated DNA molecules.

Interestingly, at low protein to DNA ratios (20 and 30% of saturation) the DNA molecules with intermediate binding densities slowly redistribute to form fully saturated DNA and free DNA as indicated by the appearance of corresponding more distinct and sharp bands on the gel (see Figure 6D). Similar experiments performed for the same protein to DNA ratios in 0.3M NaCl (Figure 6C) show the same random distributions independent of incubation time. Therefore, it appears that *Dr*SSB is able to bind to M13ssDNA with either very low cooperativity at high salt (0.3M NaCl), but with much higher cooperativity at lower salt concentrations of 0.02M. This behavior is similar to that observed for *Eco*SSB However it is important to point out that in the case of *Eco*SSB the highly cooperative complexes formed at low salt are metastable and slowly redistribute to random low cooperative complexes (33), while *Dr*SSB does show the opposite trend, indicative of high stability of its cooperative complexes.

DISCUSSION

The dimeric *Dr*SSB protein has a four OB-fold structural organization (two OB folds per subunit) (23) that is similar to its *Eco*SSB bacterial analog. Although the latter forms homotetramers with one OB-fold per subunit (9,10) they both possess four OB-folds that can provide potential sites for interaction with ssDNA. Structural similarities aside, certain differences observed in the crystal structures of these proteins may affect their interaction with ssDNA. First, *Dr*SSB possesses a structural asymmetry arising from sequence differences between its N- and C-terminal OB domains. In fact, the *Dr*SSB polypeptide sequence of the C-terminal OB-fold shares more homology to the OB-fold in *Eco*SSB as compared with the N-terminal OB-fold (23). This raises the possibility that the affinity of the N- and C- terminal OB-folds of *Dr*SSB for ssDNA can differ. Another observation that originates from the analysis of the crystal structure is that the orientation of the two monomers in *Dr*SSB places its OB-folds in positions different from that seen in the *Eco*SSB tetrameric structure. In order to fit the *Eco*SSB arrangement, one of the *Dr*SSB monomers would need to be rotated ≈40° relative to the other (23). Moreover, inspection of the protein-protein interfaces in the crystal structures of *Dr*SSB reveals a large interaction surface linking neighboring dimers through β-hairpin connectors and the N-terminal OB-folds of adjacent molecules (23). The latter interactions have been suggested as potentially responsible for cooperative interactions between *Dr*SSB molecules. However, those interactions are not observed in the *Eco*SSB crystal structures. Therefore, based on the observed differences in crystal structures, it is possible that the ssDNA

binding affinities, cooperativities and modes of ssDNA binding and wrapping may differ for these two proteins and display a different dependence on solution conditions.

DrSSB-ssDNA binding mode transition and intra-dimer negative cooperativity

At moderate and high salt conditions (≥0.2M NaCl) *Eco*SSB forms an $(SSB)_{65}$ binding mode (occluded site size ~65 nucleotides) in which ssDNA wraps around all four subunits (OB folds) of the tetramer, whereas at low salt concentrations (≤20mM NaCl) and high protein-DNA binding ratios *Eco*SSB binds to ssDNA in highly cooperative $(SSB)_{35}$ binding mode in which on average only two subunits of the tetramer (2 OB folds) interact with ssDNA (5,27,33,35, 36,38,46). In this latter mode ~65–70 nucleotides of ssDNA can accommodate two EcoSSB tetramers, which bind with positive cooperativity (27).

We show here that *Dr*SSB does undergo a small change in its occluded ssDNA binding site size as a function of [NaCl], although the change is not as extreme as the ssDNA binding mode transition observed with EcoSSB (27,35,36,46). At moderate and high NaCl concentrations (from 0.1M to 1M) the occluded site size of *Dr*SSB on poy(dT) is 50–53 nucleotides with a Trp fluorescence quenching of ~ 82%, which agrees well with the contact site size (m≈52) determined by ITC (Fig. 4). However, this is significantly smaller than the high [NaCl] induced occluded site size of 65 nucleotides determined for the *Eco*SSB tetramer (> 0.2 M NaCl). However, it is interesting to note that the *Eco*SSB tetramer displays a more similar occluded site size of ~56 nucleotides on poly(dT) at intermediate [NaCl] (40 – 100 mM) as well as intermediate $[MgCl_2]$ (3 – 60 mM) (36).

At lower NaCl concentrations ((≤20mM), *Dr*SSB displays both a lower extent of Trp fluorescence quenching and lower occluded site size (Q_{max}≈0.72–0.76 and n≈45) upon binding to poly(dT) as also observed at 1mM NaCl by Witte et al. (52). However, this is still much larger than the low salt site size of ~35 nucleotides observed for *Eco*SSB (35,36,46). Further evidence that *Dr*SSB dimers do not adopt a very small site size mode at lower [NaCl] is that only one *Dr*SSB dimer is observed to bind to oligonucleotides ($(dT)_L$) with lengths of 45–55 nucleotides. However, the observed difference in site size (45 vs. 52 nucleotides) and fluorescence quenching (0.72–0.76 vs. 0.83) for the DrSSB dimers binding to ssDNA may result from either a difference in ssDNA wrapping or a difference in cooperative interactions or both.

The *Dr*SSB binding affinity for ssDNA is strongly dependent on oligodeoxynucleotide length. Under moderate salt concentrations *Dr*SSB binds stoichiometrically to only one molecule of $(dT)_L$ if *L* is in the range from 40 to 60 nucleotides. For these oligonucleotides both the Trp fluorescence quenching and enthalpy change increases (in magnitude) with increasing oligonucleotide length up to n≈50–55 and does not increase further (Q_{max}≈83% and ΔH_{obs} ≈-94±4 kcal/mole). This can be compared to values of Q_{max}≈90% (41) and $\Delta H_{obs} \approx -130$ kcal/mol (44) for *Eco*SSB binding to $(dT)_{65}$. We note that the same extent of Trp fluorescence quenching is observed for *Dr*SSB binding to $(dT)_L$ at both low and high NaCl concentrations (with a maximum of 83–85% quenching for *L* >50 nucleotides), whereas a [NaCl]-dependence of Trp quenching is observed for *Dr*SSB binding to poly(dT) (increasing from 72–76% to 84%). This suggests that there are [NaCl] dependent effects on *Dr*SSB binding to poly(dT) that are not observed for oligodeoxynucleotide binding. This could reflect effects on the binding mode and/or cooperativity of *Dr*SSB binding to longer ssDNA.

It is also clear from our data that the binding affinity of ssDNA for *Dr*SSB is weaker than for *Eco*SSB. This is emphasized by the fact that the binding constant for oligonucleotides with a length close to its site size is measurable for *Dr*SSB at a [NaCl] concentration of 1M, whereas the binding to *Eco*SSB is still stoichiometric up to 3.0 M NaCl (41). The binding of a second *Dr*SSB dimer (although with much lower affinity) is detectable only on $(dT)_{70}$ (Fig. 4), an

oligo that provides 20 additional nucleotides for interaction with the protein, which is in good agreement with results from previous electrophoretic mobility shift assays (25). On the other hand the *Dr*SSB dimer is able to bind a second molecule of ssDNA if its length is below 35 nucleotides. Furthermore, just as for *Eco*SSB, the binding of a second molecule of such a shorter oligonucleotide occurs with a significant negative cooperativity that increases with decreasing salt concentration, just as for *Eco*SSB (41,42,53).

DrSSB forms stable highly cooperative complexes on ssDNA at low [NaCl]

Agarose gel electrophoresis have shown that at low salt concentrations (20mM NaCl) *Eco*SSB can form highly cooperative complexes on ssDNA characterized by a nonrandom distributions of *Eco*SSB bound to M13ssDNA (33). However, at higher [NaCl] (0.3M) *Eco*SSB was bound to the ssDNA population in a more random distribution indicative of low or non-cooperative binding. Our experiments with *Dr*SSB performed at the same salt conditions show very similar patterns (Fig.5) indicating that at low salt (20 mM NaCl) *Dr*SSB binds to ssDNA cooperatively, whereas at higher [NaCl], a low cooperativity binding distribution is observed. However, in contrast to the *Eco*SSB behavior, the *Dr*SSB-ssDNA complexes remain stable and do not redistribute with time to the lower cooperativity complexes. These results contrast with the sedimentation velocity results of Witte et al. (52) who reported that cooperative complexes of DrSSB on poly(dT) are metastable. Analysis of *Dr*SSB crystal structures obtained in different solution conditions reveals a large interaction surface that links neighboring dimers and comprises β-hairpin connectors and N-terminal OB domains of adjacent molecules (23). This interface includes a number of van der Waal's, hydrogen and ionic interactions and is different from the L_{45} loop mediated interface that links EcoSSB tetramers (10). Although it is still not clear whether the inter-tetramer interfaces observed in the crystal structures represent the cooperative interactions that exist when bound to ssDNA, these differences raise the possibility that the cooperative complexes formed on ssDNA with *Eco*SSB vs *Dr*SSB may be distinct with different numbers of OB folds involved in ssDNA wrapping.

Thermodynamics of DrSSB interaction with oligo(dT)

The thermodynamics of *Eco*SSB binding to ssDNA is quite complex and was studied extensively using ITC (32,43–45,54). The binding of *Eco*SSB tetramer to ssDNA is stoichiometric under most of the conditions and is characterized by an extremely large and negative enthalpy change (up to −160 kcal/mol (32), the largest enthalpy reported so far for protein-DNA interactions) and a large and negative heat capacity change, $\Delta Cp,_{obs}$ (up to −1.2 kcal/mol °K (44)). This thermodynamics is explained in large measure by multiple contributions from linked equilibrium reactions that accompany SSB-DNA binding. Among these the effects of salt concentration and type (32,43,44), protonation (45), conformational transitions within DNA (54) and protein (44) have been quantified.

Using ITC we find that at moderate salt concentrations (0.2M NaCl) *Dr*SSB binds to oligodeoxythymidylates with a contact site size of ~52 nucleotides and is characterized by a large and negative ΔH_{obs}= −94+4 kcal/mole, although both of these are significantly smaller than has been measured for *EcoSSB* (≈ −130 kcal/mole, n=65) under the same conditions (44). Interestingly, the values of ΔH_{obs} for these two proteins are similar if normalized by their respective contact sizes (−1.8 and −2.0 kcal/mol nucleotide). The dependence of ΔH_{obs} on [NaCl] for *Dr*SSB-$(dT)_{45}$ binding shows nonlinear behavior (Fig. 5A) with the largest effect at 1M NaCl. This behavior is analogous to that observed for *Eco*SSB and related to contribution to observed enthalpy change due to anion release from the protein upon interaction with ssDNA (32,44), which also affects $\Delta Cp,_{obs}$ (44). Temperature dependence of ΔH_{obs} for *Dr*SSB obtained at 0.2M NaCl (Fig.5B) provides an estimate of heat capacity change $\Delta Cp,_{obs}$= −0.29 +0.07 kcal mol^{-1} K^{-1}, which is significantly lower than the value $\Delta Cp,_{obs}$≈ −1.3 kcal mol^{-1} K^{-1} for *Eco*SSB-$(dT)_{70}$ binding under the same conditions (44). A large part of the heat

capacity change measured for *Eco*SSB is due to contributions from protonation (~ −0.5 kcal mol^{-1} K^{-1}) and the effects of salt (~ -(0.2–0.3) kcal mol^{-1} K^{-1}). The remaining contribution ~ -(0.5–0.6) kcal mol^{-1} K^{-1}, that likely reflects changes in accessible surface area upon complexation, but may have contributions from protein conformational changes (44), is still almost twice as large as the total heat capacity change measured here for *Dr*SSB. In the absence of a more detailed investigation, it is not possible to understand the origins of the lower value of ΔCp observed for *Dr*SSB, since this could result from a combination of a number of factors such as differences in accessible surface area, vibrational modes hydration or other coupled equilibria.

Abbreviations

drSSB	*Deinococcus radiodurans* Single Stranded DNA Binding protein
ssDNA	single stranded DNA
ITC	isothermal titration calorimetry
Tris	tris(hydroxymethyl)aminomethane
EDTA	ethylenediaminetetraacetic acid

Acknowledgments

We thank T. Ho for the synthesis and purification of all oligodeoxynucleotides.

REFERENCES

1. Chase JW, Williams KR. Single-stranded DNA binding proteins required for DNA replication. Annu Rev Biochem 1986;55:103–136. [PubMed: 3527040]
2. Meyer RR, Laine PS. The single-stranded DNA-binding protein of Escherichia coli. Microbiol Rev 1990;54:342–380. [PubMed: 2087220]
3. Lohman TM, Ferrari ME. Escherichia coli single-stranded DNA-binding protein: multiple DNA-binding modes and cooperativities. Annu Rev Biochem 1994;63:527–570. [PubMed: 7979247]
4. Shereda RD, Kozlov AG, Lohman TM, Cox MM, Keck JL. SSB as an organizer/mobilizer of genome maintenance complexes. Crit Rev Biochem Mol Biol 2008;43:289–318. [PubMed: 18937104]
5. Roy R, Kozlov AG, Lohman TM, Ha T. Dynamic structural rearrangements between DNA binding modes of E. coli SSB protein. J Mol Biol 2007;369:1244–1257. [PubMed: 17490681]
6. Roy R, Kozlov AG, Lohman TM, Ha T. SSB protein diffusion on single-stranded DNA stimulates RecA filament formation. Nature 2009;461:1092–1097. [PubMed: 19820696]
7. Alberts B, Frey L, Delius H. Isolation and characterization of gene 5 protein of filamentous bacterial viruses. J Mol Biol 1972;68:139–152. [PubMed: 4115107]
8. Kowalczykowski SC, Lonberg N, Newport JW, von Hippel PH. Interactions of bacteriophage T4-coded gene 32 protein with nucleic acids. I. Characterization of the binding interactions. J Mol Biol 1981;145:75–104. [PubMed: 7265204]
9. Raghunathan S, Ricard CS, Lohman TM, Waksman G. Crystal structure of the homo-tetrameric DNA binding domain of Escherichia coli single-stranded DNA-binding protein determined by multiwavelength x-ray diffraction on the selenomethionyl protein at 2.9-A resolution. Proc Natl Acad Sci U S A 1997;94:6652–6657. [PubMed: 9192620]
10. Raghunathan S, Kozlov AG, Lohman TM, Waksman G. Structure of the DNA binding domain of E-coli SSB bound to ssDNA. Nat Struct Biol 2000;7:648–652. [PubMed: 10932248]
11. Savvides SN, Raghunathan S, Futterer K, Kozlov AG, Lohman TM, Waksman G. The C-terminal domain of full-length E-coli SSB is disordered even when bound to DNA. Protein Sci 2004;13:1942–1947. [PubMed: 15169953]

12. Wold MS. Replication protein A: a heterotrimeric, single-stranded DNA-binding protein required for eukaryotic DNA metabolism. Annu Rev Biochem 1997;66:61–92. [PubMed: 9242902]
13. Iftode C, Daniely Y, Borowiec JA. Replication protein A (RPA): the eukaryotic SSB. Crit Rev Biochem Mol Biol 1999;34:141–180. [PubMed: 10473346]
14. Murzin AG. OB(oligonucleotide/oligosaccharide binding)-fold: common structural and functional solution for non-homologous sequences. EMBO J 1993;12:861–867. [PubMed: 8458342]
15. Suck D. Common fold, common function, common origin? Nat Struct Biol 1997;4:161–165. [PubMed: 9164449]
16. Purnapatre K, Handa P, Venkatesh J, Varshney U. Differential effects of single-stranded DNA binding proteins (SSBs) on uracil DNA glycosylases (UDGs) from Escherichia coli and mycobacteria. Nucleic Acids Res 1999;27:3487–3492. [PubMed: 10446237]
17. Saikrishnan K, Jeyakanthan J, Venkatesh J, Acharya N, Sekar K, Varshney U, Vijayan M. Structure of Mycobacterium tuberculosis single-stranded DNA-binding protein. Variability in quaternary structure and its implications. J Mol Biol 2003;331:385–393. [PubMed: 12888346]
18. Saikrishnan K, Manjunath GP, Singh P, Jeyakanthan J, Dauter Z, Sekar K, Muniyappa K, Vijayan M. Structure of Mycobacterium smegmatis single-stranded DNA-binding protein and a comparative study involving homologus SSBs: biological implications of structural plasticity and variability in quaternary association. Acta Crystallogr D Biol Crystallogr 2005;61:1140–1148. [PubMed: 16041080]
19. Chan KW, Lee YJ, Wang CH, Huang H, Sun YJ. Single-stranded DNA-binding protein complex from Helicobacter pylori suggests an ssDNA-binding surface. J Mol Biol 2009;388:508–519. [PubMed: 19285993]
20. Dabrowski S, Olszewski M, Piatek R, Brillowska-Dabrowska A, Konopa G, Kur J. Identification and characterization of single-stranded-DNA-binding proteins from Thermus thermophilus and Thermus aquaticus - new arrangement of binding domains. Microbiology 2002;148:3307–3315. [PubMed: 12368464]
21. Fedorov R, Witte G, Urbanke C, Manstein DJ, Curth U. 3D structure of Thermus aquaticus single-stranded DNA-binding protein gives insight into the functioning of SSB proteins. Nucleic Acids Res 2006;34:6708–6717. [PubMed: 17148487]
22. Eggington JM, Haruta N, Wood EA, Cox MM. The single-stranded DNA-binding protein of Deinococcus radiodurans. BMC Microbiol 2004;4:2. [PubMed: 14718065]
23. Bernstein DA, Eggington JM, Killoran MP, Misic AM, Cox MM, Keck JL. Crystal structure of the Deinococcus radiodurans single-stranded DNA-binding protein suggests a mechanism for coping with DNA damage. Proc Natl Acad Sci U S A 2004;101:8575–8580. [PubMed: 15159541]
24. Battista JR. Against all odds: the survival strategies of Deinococcus radiodurans. Annu Rev Microbiol 1997;51:203–224. [PubMed: 9343349]
25. Eggington JM, Kozlov AG, Cox MM, Lohman TM. Polar destabilization of DNA duplexes with single-stranded overhangs by the Deinococcus radiodurans SSB protein. Biochemistry 2006;45:14490–14502. [PubMed: 17128988]
26. Shan Q, Cox MM, Inman RB. DNA strand exchange promoted by RecA K72R. Two reaction phases with different Mg2+ requirements. J Biol Chem 1996;271:5712–5724. [PubMed: 8621437]
27. Ferrari ME, Bujalowski W, Lohman TM. Co-operative binding of Escherichia coli SSB tetramers to single-stranded DNA in the (SSB)35 binding mode. J Mol Biol 1994;236:106–123. [PubMed: 8107097]
28. Berkowitz SA, Day LA. Molecular weight of single-stranded fd bacteriophage DNA. High speed equilibrium sedimentation and light scattering measurements. Biochemistry 1974;13:4825–4831. [PubMed: 4429667]
29. Ferrari ME, Lohman TM. Apparent heat capacity change accompanying a nonspecific protein-DNA interaction. Escherichia coli SSB tetramer binding to oligodeoxyadenylates. Biochemistry 1994;33:12896–12910. [PubMed: 7947696]
30. Lohman TM, Mascotti DP. Nonspecific ligand-DNA equilibrium binding parameters determined by fluorescence methods. Methods Enzymol 1992;212:424–458. [PubMed: 1518458]
31. Wiseman T, Williston S, Brandts JF, Lin LN. Rapid measurement of binding constants and heats of binding using a new titration calorimeter. Anal Biochem 1989;179:131–137. [PubMed: 2757186]

32. Kozlov AG, Lohman TM. Calorimetric studies of E-coli SSB protein single-stranded DNA interactions. Effects of monovalent salts on binding enthalpy. J Mol Biol 1998;278:999–1014. [PubMed: 9600857]
33. Lohman TM, Overman LB, Datta S. Salt-dependent changes in the DNA binding co-operativity of Escherichia coli single strand binding protein. J Mol Biol 1986;187:603–615. [PubMed: 3519979]
34. McGhee JD, von Hippel PH. Theoretical aspects of DNA-protein interactions: co-operative and non-co-operative binding of large ligands to a one-dimensional homogeneous lattice. J Mol Biol 1974;86:469–489. [PubMed: 4416620]
35. Lohman TM, Overman LB. Two binding modes in Escherichia coli single strand binding protein-single stranded DNA complexes. Modulation by NaCl concentration. J Biol Chem 1985;260:3594–3603. [PubMed: 3882711]
36. Bujalowski W, Lohman TM. Escherichia coli single-strand binding protein forms multiple, distinct complexes with single-stranded DNA. Biochemistry 1986;25:7799–7802. [PubMed: 3542037]
37. Chrysogelos S, Griffith J. Escherichia coli single-strand binding protein organizes single-stranded DNA in nucleosome-like units. Proc Natl Acad Sci U S A 1982;79:5803–5807. [PubMed: 6764531]
38. Griffith JD, Harris LD, Register J 3rd. Visualization of SSB-ssDNA complexes active in the assembly of stable RecA-DNA filaments. Cold Spring Harb Symp Quant Biol 1984;49:553–559. [PubMed: 6397310]
39. Bujalowski W, Overman LB, Lohman TM. Binding mode transitions of Escherichia coli single strand binding protein-single-stranded DNA complexes. Cation, anion, pH, and binding density effects. J Biol Chem 1988;263:4629–4640. [PubMed: 3280566]
40. Kumaran S, Kozlov AG, Lohman TM. Saccharomyces cerevisiae replication protein A binds to single-stranded DNA in multiple salt-dependent modes. Biochemistry 2006;45:11958–11973. [PubMed: 17002295]
41. Bujalowski W, Lohman TM. Negative co-operativity in Escherichia coli single strand binding protein-oligonucleotide interactions. I. Evidence and a quantitative model. J Mol Biol 1989;207:249–268. [PubMed: 2661832]
42. Bujalowski W, Lohman TM. Negative co-operativity in Escherichia coli single strand binding protein-oligonucleotide interactions. II. Salt, temperature and oligonucleotide length effects. J Mol Biol 1989;207:269–288. [PubMed: 2661833]
43. Lohman TM, Overman LB, Ferrari ME, Kozlov AG. A highly salt-dependent enthalpy change for Escherichia coli SSB protein-nucleic acid binding due to ion-protein interactions. Biochemistry 1996;35:5272–5279. [PubMed: 8611514]
44. Kozlov AG, Lohman TM. Effects of monovalent anions on a temperature-dependent heat capacity change for Escherichia coli SSB tetramer binding to single-stranded DNA. Biochemistry 2006;45:5190–5205. [PubMed: 16618108]
45. Kozlov AG, Lohman TM. Large contributions of coupled protonation equilibria to the observed enthalpy and heat capacity changes for ssDNA binding to Escherichia coli SSB protein. Proteins Suppl 2000;4:8–22.
46. Lohman, TM.; Bujalowski, W. *E. coli* SSB protein: multiple binding modes and cooperativities. In: Revzin, A., editor. The Biology of Nonspecific DNA-Protein Interactions. CRC Press; 1990. p. 131-170.
47. Bujalowski W, Lohman TM. Limited co-operativity in protein-nucleic acid interactions. A thermodynamic model for the interactions of Escherichia coli single strand binding protein with single-stranded nucleic acids in the "beaded", (SSB)65 mode. J Mol Biol 1987;195:897–907. [PubMed: 3309344]
48. Overman LB, Bujalowski W, Lohman TM. Equilibrium binding of Escherichia coli single-strand binding protein to single-stranded nucleic acids in the (SSB)65 binding mode. Cation and anion effects and polynucleotide specificity. Biochemistry 1988;27:456–471. [PubMed: 3280021]
49. Kowalczykowski SC, Paul LS, Lonberg N, Newport JW, McSwiggen JA, von Hippel PH. Cooperative and noncooperative binding of protein ligands to nucleic acid lattices: experimental approaches to the determination of thermodynamic parameters. Biochemistry 1986;25:1226–1240. [PubMed: 3486003]

50. Bujalowski W, Lohman TM, Anderson CF. On the cooperative binding of large ligands to a one-dimensional homogeneous lattice: the generalized three-state lattice model. Biopolymers 1989;28:1637–1643. [PubMed: 2775853]

51. Epstein IR. Cooperative and non-cooperative binding of large ligands to a finite one-dimensional lattice. A model for ligand-oligonucleotide interactions. Biophys Chem 1978;8:327–339. [PubMed: 728537]

52. Witte G, Urbanke C, Curth U. Single-stranded DNA-binding protein of Deinococcus radiodurans: a biophysical characterization. Nucleic Acids Res 2005;33:1662–1670. [PubMed: 15781492]

53. Lohman TM, Bujalowski W. Negative cooperativity within individual tetramers of Escherichia coli single strand binding protein is responsible for the transition between the (SSB)35 and (SSB)56 DNA binding modes. Biochemistry 1988;27:2260–2265. [PubMed: 3289611]

54. Kozlov AG, Lohman TM. Adenine base unstacking dominates the observed enthalpy and heat capacity changes for the Escherichia coli SSB tetramer binding to single-stranded oligoadenylates. Biochemistry 1999;38:7388–7397. [PubMed: 10353851]

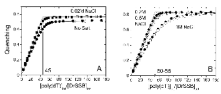

Figure 1.

Determination of occluded site size of DrSSB on poly(dT) at different NaCl concentrations (Buffer T, pH 8.1, 25°C). (A) - Results of fluorescence titrations of DrSSB (0.07μM – open squares; 0.2μM - closed squares) with poly(dT) in 0.02M NaCl and in the absence of salt (0.07μM – open circles; 0.2μM - closed circles). (B) - Results of fluorescence titrations of DrSSB with poly(dT) in 0.2 M NaCl (0.07μM – open diamonds; 0.2μM - closed diamonds), 0.5M NaCl (0.1 μM open triangles) and in 1.0 M NaCl (0.1μM – open circles; 0.2μM - closed circles). The linear increase in relative quenching indicates stoichiometric binding of the protein to poly(dT) until the point of saturation (plateau value) is reached. The occluded site sizes were determined by extrapolation of the linear parts of the titration curves to the point of intersection with the corresponding plateau value as described (35) and yields n≈45 nucleotides per DrSSB dimer (panel A) and n≈50–55 per DrSSB dimer (panel B). For the concentration of [NaCl]= 1M the binding is not stoichiometric, so the determination of the occluded site size is not posssible.

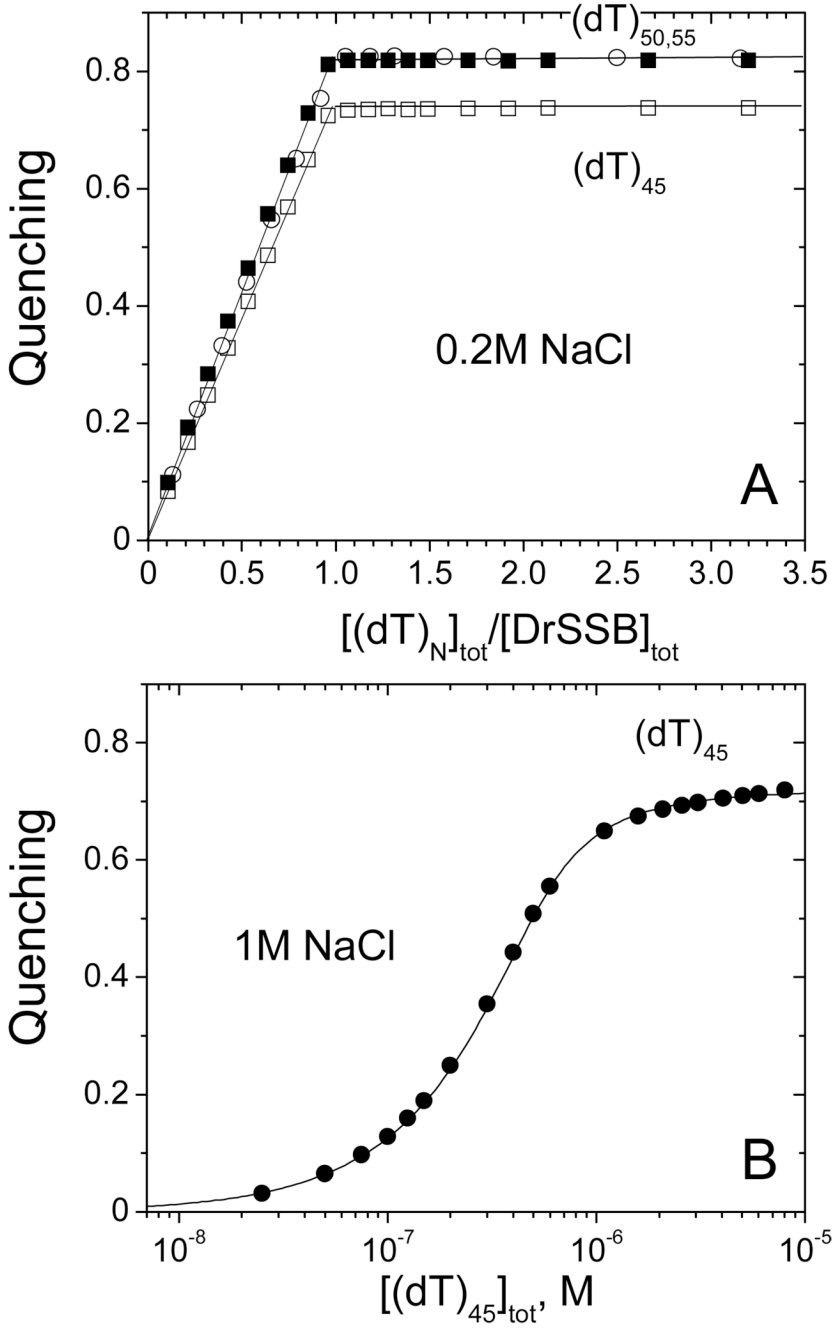

Figure 2.

Determination of occluded site size of DrSSB using oligonucleotides of different length (Buffer T, pH 8.1, 25°C). (A) - Results of fluorescence titrations of DrSSB (~1μM) with $(dT)_{45}$, $(dT)_{50}$ and $(dT)_{55}$ in the presence of 0.2M NaCl. (B) - Fluorescence titration of DrSSB (~1μM) with $(dT)_{45}$, in 1.0 M NaCl. The smooth curve represents the best fit of the data to a 1:1 model (see eq. 1 in Materials and Methods) with n=0.98±0.01, Qmax=0.72±0.01 and K_{obs}=(1.48 ±0.06)×10^7 M^{-1}.

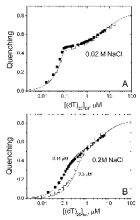

Figure 3.

DrSSB binds two molecules of $(dT)_{25}$ with negative cooperativity, which decreases with increasing salt concentration (Buffer T, pH 8.1, 25°C). (A) – Two titration of DrSSB (0.1μM (open and closed squares) with $(dT)_{25}$ 0.02M NaCl. Solid curve represent the result of global nonlinear least squares fitting of both sets of data to a two site model (eq, 2 in Materials and Methods) with best fit parameters: Q_1 = 0.48±0.01, $K_{1,obs}$ =(4.5±6.2)×10^9 M^{-1}, $K_{2,obs}$ =(1.4 ±0.1)×10^5 M^{-1} (value of Q_2=0.83 was fixed according to maximum quenching observed in poly(dT) and $(dT)_L$ experiments). (B) - Titration of DrSSB (0.14μM (closed squares) and 0.5μM (open squares)) with $(dT)_{25}$ in 0.2M NaCl. Solid curves represent the result of global nonlinear least squares fitting of both sets of data to the two site model (eq, 2 in materials and Methods) with best fit parameters: Q_1 = 0.51±0.01, $K_{1,obs}$ =(3.1±0.6)×10^7 M^{-1}, $K_{,obs}$ =(2.1 ±0.3)×10^5 M^{-1} (value of Q_2=0.83 was fixed according to maximum quenching observed in poly(dT) and $(dT)_L$ experiments).

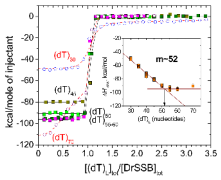

Figure 4.

Determination of the contact site size of DrSSB and corresponding binding enthalpy using ITC titrations of DrSSB with $(dT)_L$ (L=30,35,40,45, 50 55 60 and 70) in 0.1M NaCl (Buffer T, pH 8.1, 25°C). The insert shows the decrease in binding ehthalpy with increasing of oligonucleotide length until the number of nucleotides corresponding to the contact site size (m≈52) is reached. The binding enthalpy ΔH_{obs}=94±4 kcal/mol was estimated from the plateau value as an average for DrSSB titrations with $(dT)_{55}$, $(dT)_{60}$ and $(dT)_{70}$. In the case of $(dT)_{30}$ and $(dT)_{70}$ (open circles and triangles) the shape of the isotherms indicate weak binding the second ssDNA molecule to DrSSB dimer and second DrSSB dimer to ssDNA, respectively. The reliable estimates for the binding of one ssDNA to one DrSSB dimer ($K_{1,obs}$ and $\Delta H_{1,obs}$) can be obtained for either case fitting the data to a two-sequential sites binding model (eq 4 in Materials and Methods). The solid curve through experimental data points represents simulation based on the best fit parameters.

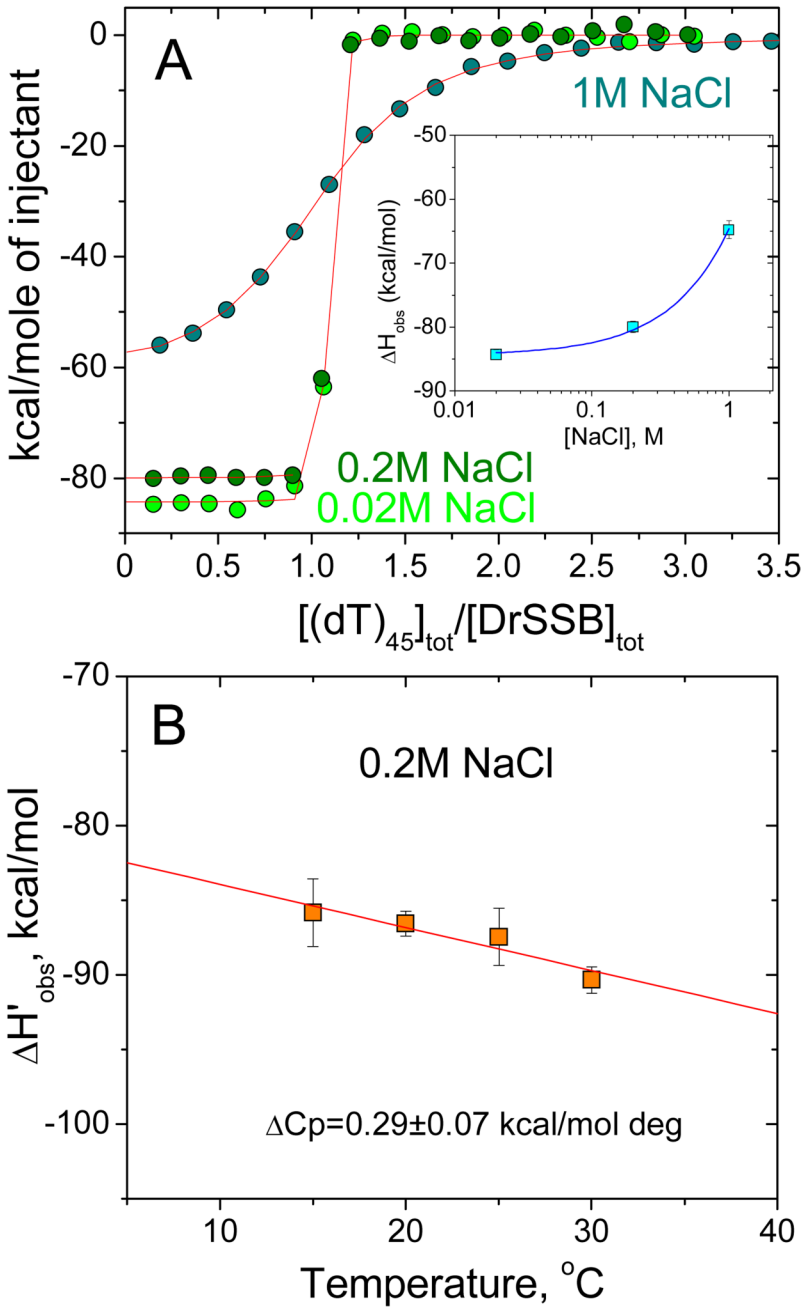

Figure 5.

The effects of salt concentration and temperature on the observed enthalpy change for DrSSB binding to $(dT)_{45}$. (A) – ITC titrations of DrSSB with $(dT)_{45}$ in Tris buffer, pH 8.1 at 0.02 (green), 0.2 (olive) and 1M NaCl (cyan). Solid curves represent the fits to a 1:1 binding model (see eq. 3 in Materials and Methods). The binding is stoichiometric at 0.02 and 0.2M NaCl so only the values of ΔH_{obs} can be determined, although in 1M NaCl all binding parameters (n=0.99±0.01, $K_{obs}=(1.66\pm0.14)\times10^7$ M^{-1} and of ΔH_{obs} = −64.8±1.4 kcal/mol) can be estimated. The dependence of ΔH_{obs} on [NaCl] is shown in the insert. (B) – the dependence of ΔH_{obs} on temperature obtained within the range from 15 to 30°C in Phosphate buffer, (pH

7.5, 0.2M NaCl). The value of ΔCp_{obs} =0.29±0.07 kcal/mol deg was determined from the linear least square fit of the data.

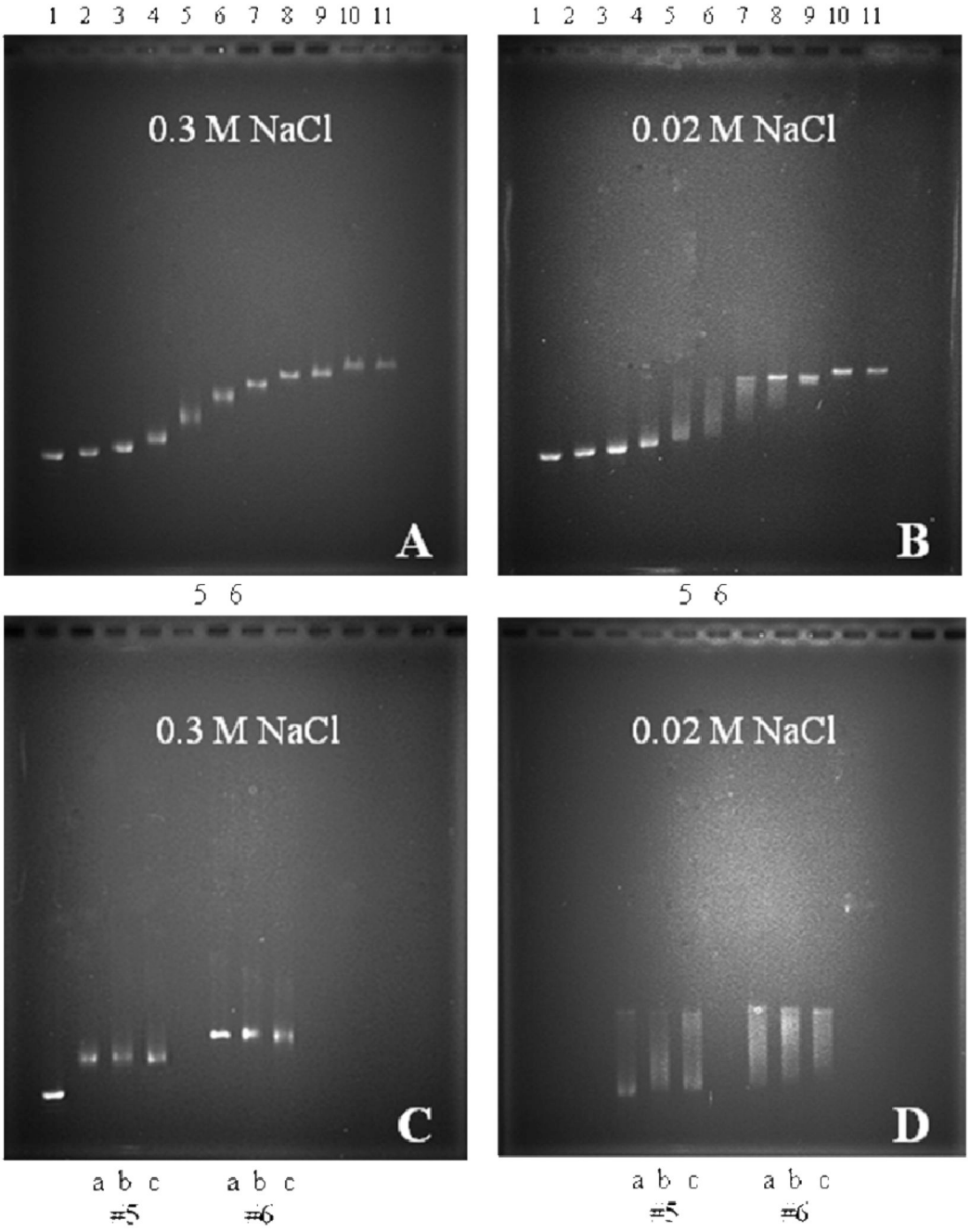

Figure 6.

Electrophoresis of DrSSB-M13ssDNA complexes (buffer T, pH 8.1, 22°C) shows that at low salt concentration DrSSB forms stable cooperative complexes on ssDNA. The complexes were formed adding DrSSB to single stranded M13mp8 at different protein to ssDNA ratios: R=0 (free DNA) (#1), R=0.025 (#2), R=0.05 (#3), R=0.1 (#4), R=0.2 (#5), R=0.3 (#6), R=0.4 (#7), R=0.5 (#8), R=0.6 (#9), R=0.8 (#10) and R=1.0 (#11). The ratios R=n×(DrSSB(dimer)/ nucleotide), were calculated using site size n=45 and n=50 nucleotides per dimer for 0.02M and 0.3M NaCl, respectively. (A) – 0.3M NaCl, gel patterns show only single band at all protein DNA ratios indicative of low cooperative binding; (B) – 0.02 M NaCl, non-random distribution of protein among the DNA molecules (lanes #4–8) is indicative of cooperative binding; (C) –

noncooperative complexes in 0.3M NaCl (R=0.2 (#5) and R=0.3 (#6)) after different preincubation times: 18 hours (a), 2 hours (b) and 10 minutes (c); (D) – cooperative complexes formed in 0.02M NaCl (all conditions as in (C)).

Table 1

Results of Equilibrium Titrations of DrSSB with ssDNA Monitoring Trp Fluorescence Quenching[a].

[NaCl]	Poly(dT)			$(dT)_{50}$ (1:1)		$(dT)_{45}$ (1:1)		$(dT)_{25}$ (2:1)	
	N^b (nts)	Q_{max}	K_{obs},[c] (M^{-1})	Q_{max}	K_{obs},[c] (M^{-1})	Q_{max}	K_{obs}, (M^{-1})[c]	Q_1, Q_2	$K_{1,obs}$ (M^{-1}),[c] $K_{2,obs}$ (M^{-1})
no salt	46	0.72	st	-	-	-	-	-	-
0.02 M	45	0.76	st	0.84	st	0.76	st	0.48±0.01 0.83(fixed)	$(4.5\pm6.2)\times10^9$ $(1.4\pm0.1)\times10^5$
0.2 M	50	0.84	st	0.83	st	0.76	st	0.51±0.01 0.83(fixed)	$(3.1\pm0.6)\times10^7$ $(2.1\pm0.3)\times10^5$
0.5 M	55	0.83	st	-	-	-	-	-	-
1.0 M	N/A	0.84	N/A	-	-	0.72	$(1.5\pm0.1)\times10^7$	-	-

[a] Solution conditions: 10mM Tris (pH 8.1), 0.1 mM EDTA.

[b] Occluded site size in nucleotides determined as described in the text.

[c] st – stoichiometric binding; the errors are shown as S.D.